Potent, Orally Bioavailable Diazabicyclic Small-Molecule Mimetics of Second Mitochondria-derived Activator of Caspases

Yuefeng Peng[+], **Haiying Sun**[+], **Zaneta Nikolovska-Coleska**[+], **Su Qiu**[+], **Chao-Yie Yang**[+], **Jianfeng Lu**[+], **Qian Cai**[+], **Han Yi**[+], **Sanmao Kang**, **Dajun Yang**, and **Shaomeng Wang**[+,*]

+*Comprehensive Cancer Center and Departments of Internal Medicine, Pharmacology and Medicinal Chemistry, University of Michigan, 1500 E. Medical Center Drive, Ann Arbor, MI 48109, USA; Ascenta Therapeutics, Inc. 101 Lindenwood Drive, Suite 405, Malvern, PA 19355, USA*

Abstract

A series of small-molecule Smac mimetics containing a diazabicyclic core structure have been designed, synthesized and evaluated. The most potent compound (**6**) binds to XIAP, cIAP-1 and cIAP-2 with K_i values of 8.4, 1.5 and 4.2 nM, respectively, directly antagonizes XIAP in a cell-free functional assay and induces cIAP-1 degradation in cancer cells. It inhibits cell growth with an IC_{50} value of 31 nM, effectively induces apoptosis in the MDA-MB-231 cancer cell line and has a good oral bioavailability.

Introduction

Inhibitor of apoptosis proteins (IAPs)[a] are key apoptosis regulators characterized by the presence of one to three regions known as baculoviral IAP repeat (BIR) domains.[1,2] Among these IAP proteins, cellular IAP-1 (cIAP-1) and cIAP-2 play critical roles in regulation of tumor necrosis factor receptor-mediated apoptosis,[3,4] and X-linked IAP (XIAP) is a central regulator of both death-receptor-mediated and mitochondria-mediated apoptosis pathways.[5] XIAP and cIAP-1 play a role in apoptosis-resistance of cancer cells to a variety of anticancer drugs and are considered to be promising cancer therapeutic targets.[5,6]

Smac (Second Mitochondria-derived Activator of Caspases), a potent pro-apoptotic protein, is an endogenous antagonist of IAP proteins.[7,8] Previous studies have established that Smac interacts with XIAP and cIAP-1/2 proteins *via* its AVPI tetrapeptide motif.[2,9-12] In the last few years, intense research efforts have been devoted to the design and development of Smac mimetics, small molecules which mimic the AVPI binding motif and function as antagonists of IAP proteins.[13-22] Smac mimetics are considered to have the great potential to be developed as a new class of anticancer drugs by promoting apoptosis in cancer cells. Two types of Smac mimetics, monovalent and bivalent, have been reported. The monovalent compounds are designed to mimic the binding of a single AVPI binding motif to IAP proteins,[14-18] and the bivalent compounds contain two AVPI binding motif mimetics tethered together through a linker.[13,19-22] We have shown that the bivalent Smac mimetics can achieve much higher affinities to XIAP and are 1-2 orders of magnitude more potent than the corresponding monovalent Smac mimetic in induction of apoptosis in tumor cells.[19] However, because of

* To whom all correspondence should be addressed: Telephone: (734)615-0362; Fax: (734)6479647; Email: E-mail: shaomeng@umich.edu.

[a]Abbreviations: IAP, inhibitor of apoptosis protein; XIAP, X-linked IAP; cIAP-1/-2, cellular IAP 1/2; Smac, second mitochondria-derived activator of caspases; BIR, baculoviral IAP repeats (BIR) domain; BIR2, the second BIR domain; BIR3, the third BIR domain; FP, fluorescence polarization; PK, pharmacokinetics; C_{max}, maximum concentration; $T_{1/2}$, elimination half life; AUC, area-under-the-curve; PARP, poly(ADP-ribose) polymerase.

their lower molecular weights, properly designed monovalent Smac mimetics can possess major advantages over bivalent Smac mimetics for purposes of drug design.

Our laboratory has previously reported the structure-based design, synthesis and evaluation of a series of conformationally constrained monovalent Smac mimetics.[14,15,17,19] Compound **1** (Figure 1) binds to the XIAP BIR3 protein with a K_i value of 26 nM.[19] Compound **1** directly antagonizes XIAP in a cell-free functional assay and induces apoptosis in cancer cells.[19] It also binds to cIAP-1 and cIAP-2 with K_i values of 1.0 and 1.8 nM (Table 1), respectively and is thus a potent monovalent Smac mimetic.

To examine if compound **1** can be potentially a drug candidate, we evaluated its pharmacokinetics (PK) in rats. Compound **1** achieved a maximum concentration (C_{max}) of 545 $\pm$ 43 nM, an elimination half life ($T_{1/2}$) of 1.7 ± 0.3 hours and $AUC_{(0-\infty)}$ (area-under-the-curve) of 482 ± 92 μg/L*hr at 25 mg/kg administered orally and an oral bioavailability of 14%. Hence, compound **1** has a modest AUC and oral bioavailability, making it less than an ideal drug candidate for further development. To improve the PK profile, we have decided to modify the core structure of **1**, which led to a new class of Smac mimetics. The most promising new compound (**6**) binds to XIAP and cIAP-1/2 with very high affinities, is more potent than **1** in cell-based assays and has improved PK parameters and oral bioavailability as compared to **1**.

Results and Discussion

Our model of **1** complexed with XIAP BIR3 showed that while the 8-membered ring has van der Waals contacts with Trp323 in XIAP BIR3, the middle portion of this 8-membered ring is largely exposed to solvent (Figure 2). Based upon this model, we predicted that replacement of one of the carbons in the 8-membered ring atoms by a nitrogen may not be detrimental to the binding to XIAP.

To test this idea, we designed and synthesized compound **2** (Figure 1, Scheme I and II), which has a diazabicyclic core structure. This compound binds to XIAP BIR3 with a K_i value of 20 nM in our fluorescence polarization-based (FP-based) XIAP binding assay[23] and is thus as potent as **1**. It also binds to cIAP-1 and cIAP-2 with K_i values of 1.2 nM and 4.6 nM respectively, determined in FP-based competitive binding assays for these two proteins. Hence, **2** is a potent Smac mimetic and a promising compound for further optimization.

Modifications of the secondary amino nitrogen in the 8-membered ring of **2** were conducted to explore structure-activity relationships at this site. Introduction of a methyl or benzyl group on the nitrogen resulted in **3** and **4**, and introduction of an acetyl group, or a phenylacetyl group on the nitrogen atom yielded **5** and **6**, respectively.

Compounds **3** and **4** have K_i values of 341 nM and 91.8 nM to XIAP BIR3, respectively, 4-17 times weaker than compound **2**. Although both compounds bind to cIAP-1 with high affinities, they are 3 times weaker than **2**. Similarly, compounds **3** and **4** bind to cIAP-2 with affinities 2-3 times weaker than **2**.

In binding to XIAP BIR3, both **5** and **6** have higher binding affinities than **2**, with K_i values of 5.4 nM and 8.4 nM, respectively. These compounds, with K_i values of 1.3 and 1.5 nM respectively, are as potent as **2** to cIAP-1. Compound **6** is as potent and compound **5** is twice as potent as **2** in binding to cIAP-2. These binding data for compounds **2**-**6** showed that modifications at this site can significantly impact the binding affinities of these Smac mimetics to XIAP, cIAP-1 and cIAP-2 proteins.

We next evaluated if compounds **2**-**6** behave as antagonists of XIAP in cell-free functional assays. The results for three representative compounds **1**, **4** and **6** are shown in Figure 3. The

XIAP BIR3 protein effectively inhibits the activity of caspase-3/-7, and these Smac mimetics dose-dependently antagonize XIAP and restore caspase activity (Figure 3A and Supporting Information). Consistent with the binding affinities, compound **6** has twice the potency of **1** and ten times that of **4** in antagonizing XIAP in this functional assay.

Previous studies showed that Smac mimetics can effectively inhibit cell growth and induce apoptosis in the MDA-MB-231 human breast cancer cell line.[16,17] We have evaluated these new Smac mimetics for cell growth inhibition in the MDA-MB-231 cancer cell line (Figure 4) and found that while all these compounds are effective, **5** and **6**, with IC_{50} values of 69 nM and 31 nM respectively, are the two most potent; **6** is 8-times more potent than **1** in this cell growth assay. Compounds **3** and **4** are the two least potent with IC_{50} values of 1300 and 1000 nM, respectively.

We evaluated the most potent compound **6** for its ability to induce apoptosis in the MDA-MB-231 cancer cell line. Compound **6** effectively induces apoptosis in this cancer cell line in a dose- and time-dependent manner (Figure 5). For example, compound **6** at 100 nM for 24- and 48-h treatment induces 31% and 47% of the MDA-MB-231 breast cancer cells to undergo apoptosis, respectively.

Several recent studies have shown that Smac mimetics induce cIAP-1 degradation in cancer cells, mediating apoptosis induction and cIAP-1 is a direct target of Smac mimetics.[20-22] We have evaluated our Smac mimetics for their ability of to induce cIAP-1 degradation and cleavage of caspase-3 and poly(ADP-ribose) polymerase (PARP) in the MDA-MB-231 cell line. We found that **6** at concentrations as low as 10 nM effectively induces the degradation of cIAP-1 and is more potent than **1**, **2** and **4** (Figure 6). Consistent with the potent activity it showed in the apoptosis assay (Figure 5), at concentrations as low as 100 nM, **6** induces robust cleavage of PARP and processing of caspase-3, two biochemical markers of apoptosis, within 24 hours and is more effective than **1**, **2** or **4**.

We next evaluated the pharmacokinetics in rats of **6** dosed orally and found that it achieves a C_{max} of 532 ± 249 nM, a $T_{1/2}$ of 4.7 ± 2.2 hours and $AUC_{(0-\infty)}$ of 1985 ± 614 μg/L*hr at 30 mg/kg. The C_{max} value for **6** at 30 mg/kg is 17 times of its IC_{50} value in the cell growth assay in the MDA-MB-231 cancer cell line and it has an oral bioavailability of 24% at doses of 30 mg/kg in rats. In direct comparison, **6** has a longer $T_{1/2}$ and a larger AUC value than **1** and a better oral bioavailability. Hence, compound **6** has a significantly better PK profile than **1**.

The synthesis of compounds **2**-**6** is shown in Schemes I and II. Compound **7** (Scheme I) was synthesized using a published method.[24] Protection of the amino group in **7** with carbobenzoxy gave a carbamate which was treated with $SOCl_2$ in MeOH to transform the *tert*-butyl ester to a methyl ester. The primary amino group was reprotected with *t*-Boc to afford **8**, hydrolysis of whose methyl ester followed by condensation of the resulting acid with aminodiphenylmethane yielded **9**. Removal of the *t*-Boc protecting group in **9** and subsequent condensation of the resulting amine with *L-N-t*-Boc-N-methyl alanine furnished an amide. Cleavage by hydrogenation of the Cbz protecting group in this amide afforded the common key intermediate **10**.

The synthesis of compounds **2**-**6** is shown in Scheme II. Methylation or benzylation of **10** group furnished the alkylated amines and removal of the *t*-Boc protecting group in these compounds provided **3** and **4** respectively. Condensation of **10** with acetic anhydride or phenylacetyl chloride afforded the respective amides and subsequent removal of the *t*-Boc protecting group gave **5** and **6**, respectively.

Summary

A series of novel Smac mimetics have been designed and synthesized through modifications of the [8,5] bicyclic core structure in our initial compound **1**. Several new, highly potent and cell-permeable Smac mimetics were obtained. The most potent compound, **6**, binds to XIAP, cIAP-1 and cIAP-2 with K_i values of 8.4, 1.5 and 4.2 nM, respectively. Compound **6** potently inhibit cell growth in the MDA-MB-231 cell line with an IC_{50} value of 31 nM and effectively induces apoptosis at 100 nM within 24-hour treatment. Significantly, compound **6** is orally bioavailable and has excellent aqueous solubility. These data reveal that compound **6** is a promising lead compound for further evaluation and optimization. Extensive optimization and *in vitro* and *in vivo* testing of **6** and its analogues are under way and will be reported in due course.

Experimental Section

Chemistry

General Methods—NMR spectra were measured at 300 MHz. ^{1}H chemical shifts are reported relative to DHO (4.79 ppm) as internal standard. Final products were purified by C18 reverse phase semi-preparative HPLC column with solvent A (0.1% of TFA in water) and solvent B (0.1% of TFA in CH_3CN) as eluents.

(5*S*,8*S*,10a*R*)-N-Benzhydryl-5-((*S*)-2-(methylamino) propanamido)-6-oxodeca-hydropyrrolo[1,2-a][1,5] diazocine-8-carbox-amide (2)—Trifluoroacetic acid (1 mL) was added to a solution of **10** (35 mg, 0.06 mmol) in methanol (5 mL). The solution was stirred at room temperature overnight and then concentrated to give crude **2** which was purified by reverse phase semi-preparative HPLC to give pure **2** as its trifluoroacetate salt (40 mg, 95%). The gradient ran from 80% of solvent A and 20% of solvent B to 60% of solvent A and 40% of solvent B in 40 min. ^{1}HNMR (300 MHz, D_2O) δ 7.42-7.29 (m, 10H), 6.03 (d, *J* = 6.8 Hz, 1H), 5.36 (m, 1H), 4.75 (m, 1H), 4.61 (m, 1H), 3.99 (dd, *J* = 12.0, 5.4 Hz, 1H), 3.68 (m, 1H), 3.55 (m, 1H), 3.43 (m, 1H), 3.25 (m, 1H), 2.69 (s, 3H), 2.49 (m, 1H), 2.30-1.82 (m, 5H), 1.52 (d, *J* = 7.1 Hz, 3H); ESI MS: *m/z* 500.4 (M+Na)$^+$. Anal. ($C_{27}H_{35}N_5O_3$·2.7CF$_3$COOH): C, H, N.

(5*S*,8*S*,10a*R*)-N-benzhydryl-3-methyl-5-((*S*)-2-(methylamino)propanamido)-6-oxodeca-hydro pyrrolo[1,2-a][1,5]diazocine-8-carbox-amide (3)—Aqueous formaldehyde solution (37%, 0.2 mL) and HOAc (0.2 mL) were added to a solution of **10** (44 mg, 0.076 mmol) in MeOH (5 mL). After addition of NaBH$_3$CN (50 mg, 0.79 mmol) at 0°C, the solution was warmed to room temperature and stirred for 3 hours. The mixture was concentrated and then partitioned between EtOAc (20 mL) and brine (5 mL). The organic layer was dried over Na_2SO_4 and concentrated and the residue was purified by chromatography to give the methylated amine. Trifluoroacetic acid (1 mL) was added to a solution of this amine in MeOH (5 mL). The solution was stirred at room temperature overnight and then concentrated to give crude **3** which was purified by reverse phase semipreparative HPLC to give pure **3** as its trifluoroacetate salt (38 mg, 71% over two steps). The gradient ran from 75% of solvent A and 25% of solvent B to 60% of solvent A and 40% of solvent B in 40 min. ^{1}HNMR (300 MHz, D_2O) δ 7.42-7.25 (m, 10H), 6.07 (d, *J* = 6.8 Hz, 1H), 5.35 (m, 1H), 4.70 (m, 1H), 4.61 (m, 1H), 3.99 (dd, *J* = 14.0, 7.0 Hz, 1H), 3.86 (m, 1H), 3.65 (m, 1H), 3.56 (m, 1H), 3.30 (m, 1H), 3.00 (s, 3H), 2.68 (s, 3H), 2.49 (m, 1H), 2.32-1.82 (m, 5H), 1.51 (d, *J* = 7.1 Hz, 3H); ESI MS: *m/z* 492.3 (M+H)$^+$. Anal. ($C_{28}H_{37}N_5O_3$·3.1CF$_3$COOH): C, H, N.

(5*S*,8*S*,10a*R*)-N-benzhydryl-3-benzyl-5-((*S*)-2-(methylamino)propanamido)-6-oxodeca-hydropyrrolo[1,2-a][1,5]diazocine-8-carbox-amide (4)—Benzyl bromide (0.1 mL) and NaHCO$_3$ (0.3 g) were added a solution of **10** (48 mg, 0.083 mmol) in DMF (5

mL). The mixture was stirred at room temperature overnight and then concentrated before being partitioned between EtOAc (20 mL) and brine (5 mL). The organic layer was dried over Na_2SO_4 then concentrated and the residue was purified by chromatography to give a benzylated amine. To a solution of this amine in methanol (5 mL) was added trifluoroacetic acid (1 mL). The solution was stirred at room temperature overnight and then concentrated to give crude product which was purified by reverse phase semi-preparative HPLC to give pure **4** as a salt with TFA (51 mg, 77% over two steps). The gradient ran from 75% of solvent A and 25% of solvent B to 60% of solvent A and 40% of solvent B in 40 min. ^{1}HNMR (300 MHz, D_2O) δ 7.34 (m, 2H), 7.28-7.02 (m, 13H), 6.05 (d, J = 6.9 Hz, 1H), 5.38 (m, 1H), 4.72 (m, 1H), 4.52 (m, 1H), 4.25 (ABq, J = 8.4 Hz, 2H), 3.97 (dd, J = 13.5, 6.8 Hz, 1H), 3.82-3.56 (m, 2H), 3.49 (m, 1H), 3.18 (m, 1H), 2.67 (s, 3H), 2.35 (m, 1H), 2.08 (m, 1H), 1.75-1.52 (m, 4H), 1.47 (d, J = 7.0 Hz, 3H); ESI MS: m/z 568.3 $(M+H)^+$; Anal. $(C_{34}H_{41}N_5O_3 \cdot 2.9CF_3COOH)$: C, H, N.

(5*S*,8*S*,10a*R*)-3-acetyl-N-benzhydryl-5-((*S*)-2-(methylamino)propanamido)-6-oxodeca-hydro pyrrolo[1,2-a][1,5]diazocine-8-carbox-amide (5)—Acetic

anhydride (0.1 mL) and *N,N*-diisopropylethylamine (0.3 mL) were added to a solution of **10** (46 mg, 0.08 mmol) in CH_2Cl_2 (5 mL) at 0°C. The mixture was stirred at room temperature overnight, concentrated and then partitioned between EtOAc (20 mL) and brine (5 mL). The organic layer was dried over Na_2SO_4 and then concentrated. The residue was purified by chromatography to give an amide. HCl solution (4N in 1,4-dioxane, 1 mL) was added to a solution of this residue in MeOH (5 mL). The solution was stirred at room temperature overnight and then concentrated to give crude **5** which was purified by reverse phase semi-preparative HPLC to give pure product (38 mg, 85% over two steps). The gradient ran from 70% of solvent A and 30% of solvent B to 50% of solvent A and 50% of solvent B in 40 min. ^{1}HNMR (300 MHz, D_2O) δ 7.38-7.19 (m, 10H), 5.95 (brs, 1H), 4.96 (m, 1H), 4.40 (m, 1H), 4.25 (m, 1H), 3.94 (m, 1H), 3.66 (m, 1H), 3.60-3.35 (m, 3H), 2.63 (s, 3H), 2.25 (m, 1H), 2.15-1.65 (m, 8H), 1.47 (d, J = 7.1Hz, 3H); ESI MS: m/z 520.3 $(M+H)^+$; Anal. $(C_{29}H_{37}N_5O_4 \cdot 1.0HCl \cdot 1.5CF_3COOH)$: C, H, N.

(5*S*,8*S*,10a*R*)-N-Benzhydryl-5-((*S*)-2-(methyl-amino) propanamido)-6-oxo-3-(2-phenyl-acetyl)decahydro pyrrolo[1,2-a][1,5]diazo-cine-8-carboxamide (6).—

Phenylacetyl chloride (0.1 mL) and *N,N*-diisopropylethylamine (0.3 mL) were added to a solution of **10** (47 mg, 0.08 mmol) in CH_2Cl_2 (10 mL). The mixture was stirred at room temperature overnight, concentrated and then partitioned between EtOAc (20 mL) and brine (5 mL). The organic layer was dried over Na_2SO_4 then concentrated and the residue was purified by chromatography to give an amide. HCl (4N in 1,4-dioxane, 1 mL) was added to a solution of this amide in MeOH. The solution was stirred at room temperature overnight and then concentrated to give crude **6**, which was purified by reverse phase semi-preparative HPLC to give pure product (44 mg, 87% over two steps). The gradient ran from 70% of solvent A and 30% of solvent B to 50% of solvent A and 50% of solvent B in 40 min. ^{1}HNMR (300 MHz, D_2O) δ 7.27-6.90 (m, 15H), 5.95 (brs, 1H), 4.65 (m, 1H), 4.38 (m, 1H), 4.06 (m, 1H), 3.85 (m, 1H), 3.78-3.30 (m, 6H), 2.55 (brs, 3H), 2.08 (m, 1H), 1.98-1.30 (m, 8H); ESI MS: m/z 596.3 $(M+H)^+$; Anal. $(C_{35}H_{41}N_5O_4 \cdot 1.0HCl \cdot 1.2CF_3COOH)$: C, H, N.

Supplementary Material

Refer to Web version on PubMed Central for supplementary material.

Acknowledgment

Supporting Information Available: An experimental section including details of the synthesis and chemical data of intermediates, biochemical and cellular assays, molecular modeling and pharmacokinetics. This information is available free of charge *via* the Internet at http://pubs.acs.org.

References

1. Deveraux QL, Reed JC. IAP family proteins-suppressors of apoptosis. Genes Dev 1999;1:239–252. [PubMed: 9990849]

2. Salvesen GS, Duckett CS. IAP proteins: blocking the road to death's door. Nat. Rev. Mol. Cell Biol 2002;3:401–410. [PubMed: 12042762]

3. Fotin-Mleczek M, Henkler F, Samel D, Reichwein M, Hausser A, Parmryd I, Scheurich P, Schmid JA, Wajant H. Apoptotic crosstalk of TNF receptors: TNF-R2-induces depletion of TRAF2 and IAP proteins and accelerates TNF-R1-dependent activation of caspase-8. J Cell Sci 2002;115:2757–70. [PubMed: 12077366]

4. Deng Y, Ren X, Yang L, Lin Y, Wu X. A JNK-dependent pathway is required for TNFalpha-induced apoptosis. Cell 2003;115:61–70. [PubMed: 14532003]

5. Holcik M, Gibson H, Korneluk RG. XIAP: Apoptotic brake and promising therapeutic target. Apoptosis 2001;6:253–261. [PubMed: 11445667]

6. Fulda S. Inhibitor of apoptosis proteins as targets for anticancer therapy. Expert Rev Anticancer Ther 2007;7:1255–64. [PubMed: 17892425]

7. Du C, Fang M, Li Y, Li L, Wang X. Smac, a mitochondrial protein that promotes cytochrome c-dependent caspase activation by eliminating IAP inhibition. Cell 2000;102:33–42. [PubMed: 10929711]

8. Verhagen AM, Ekert PG, Pakusch M, Silke J, Connolly LM, Reid GE, Moritz RL, Simpson RJ, Vaux DL. Identification of DIABLO, a mammalian protein that promotes apoptosis by binding to and antagonizing IAP proteins. Cell 2000;102:43–53. [PubMed: 10929712]

9. Wu G, Chai J, Suber TL, Wu JW, Du C, Wang X, Shi Y. Structural basis of IAP recognition by Smac/DIABLO. Nature 2000;408:1008–1012. [PubMed: 11140638]

10. Liu Z, Sun C, Olejniczak ET, Meadows R, Betz SF, Oost T, Herrmann J, Wu JC, Fesik SW. Structural basis for binding of Smac/DIABLO to the XIAP BIR3 domain. Nature 2000;408:1004–1008. [PubMed: 11140637]

11. Srinivasula SM, Hegde R, Saleh A, Datta P, Shiozaki E, Chai J, Lee RA, Robbins PD, Fernandes-Alnemri T, Shi Y, Alnemri ES. A conserved XIAP-interaction motif in caspase-9 and Smac/DIABLO regulates caspase activity and apoptosis. Nature 2001;410:112–116. [PubMed: 11242052]

12. Shiozaki EN, Chai J, Rigotti DJ, Riedl SJ, Li P, Srinivasula SM, Alnemri ES, Fairman R, Shi Y. Mechanism of XIAP-mediated inhibition of caspase-9. Mol. Cell 2003;11:519–527. [PubMed: 12620238]

13. Li L, Thomas RM, Suzuki H, De Brabander JK, Wang X, Harran PG. A small molecule Smac mimic potentiates TRAIL- and TNFalpha-mediated cell death. Science 2004;305:1471–4. [PubMed: 15353805]

14. Sun H, Nikolovska-Coleska Z, Yang C-Y, Xu L, Liu M, Tomita Y, Pan H, Yoshioka Y, Krajewski K, Roller PP, Wang S. Structure-Based Design of Potent, Conformationally Constrained Smac Mimetics. J. Am. Chem. Soc 2004;126(51):16686–16687. [PubMed: 15612682]

15. Sun H, Nikolovska-Coleska Z, Yang CY, Xu L, Tomita Y, Krajewski K, Roller PP, Wang S. Structure-based design, synthesis, and evaluation of conformationally constrained mimetics of the second mitochondria-derived activator of caspase that target the X-linked inhibitor of apoptosis protein/caspase-9 interaction site. J Med Chem 2004;47:4147–50. [PubMed: 15293984]

16. Oost TK, Sun C, Armstrong RC, Al-Assaad AS, Betz SF, Deckwerth TL, Ding H, Elmore SW, Meadows RP, Olejniczak ET, Oleksijew A, Oltersdorf T, Rosenberg SH, Shoemaker AR, Tomaselli KJ, Zou H, Fesik SW. Discovery of potent antagonists of the antiapoptotic protein XIAP for the treatment of cancer. J Med Chem 2004;47:4417–26. [PubMed: 15317454]

17. Sun H, Nikolovska-Coleska Z, Lu J, Qiu S, Yang C-Y, Gao W, Meagher J, Stuckey J, Wang S. Design, synthesis, and evaluation of a potent, cell-permeable, conformationally constrained second mitochondria derived activator of caspase (Smac) mimetic. J Med Chem 2006;49:7916–20. [PubMed: 17181177]

18. Zobel K, Wang L, Varfolomeev E, Franklin MC, Elliott LO, Wallweber HJ, Okawa DC, Flygare JA, Vucic D, Fairbrother WJ, Deshayes K. Design, synthesis, and biological activity of a potent Smac mimetic that sensitizes cancer cells to apoptosis by antagonizing IAPs. ACS Chem Biol 2006;1:525–33. [PubMed: 17168540]

19. Sun H, Nikolovska-Coleska Z, Lu J, Meagher JL, Yang C-Y, Qiu S, Tomita Y, Ueda Y, Jiang S, Krajewski K, Roller PP, Stuckey JA, Wang S. Design, synthesis, and characterization of a potent, nonpeptide, cell-permeable, bivalent Smac mimetic that concurrently targets both the BIR2 and BIR3 domains in XIAP. J Am Chem Soc 2007;129:15279–94. [PubMed: 17999504]

20. Varfolomeev E, Blankenship JW, Wayson SM, Fedorova AV, Kayagaki N, Garg P, Zobel K, Dynek JN, Elliott LO, Wallweber HJ, Flygare JA, Fairbrother WJ, Deshayes K, Dixit VM, Vucic D. IAP antagonists induce autoubiquitination of c-IAPs, NF-kappaB activation, and TNFalpha-dependent apoptosis. Cell 2007;131:669–81. [PubMed: 18022362]

21. Vince JE, Wong WW, Khan N, Feltham R, Chau D, Ahmed AU, Benetatos CA, Chunduru SK, Condon SM, McKinlay M, Brink R, Leverkus M, Tergaonkar V, Schneider P, Callus BA, Koentgen F, Vaux DL, Silke J. IAP antagonists target cIAP1 to induce TNFalpha-dependent apoptosis. Cell 2007;131:682–93. [PubMed: 18022363]

22. Petersen SL, Wang L, Yalcin-Chin A, Li L, Peyton M, Minna J, Harran P, Wang X. Autocrine TNFalpha signaling renders human cancer cells susceptible to Smac-mimetic-induced apoptosis. Cancer Cell 2007;12:445–56. [PubMed: 17996648]

23. Nikolovska-Coleska Z, Wang R, Fang X, Pan H, Tomita Y, Li P, Roller PP, Krajewski K, Saito NG, Stuckey JA, Wang S. Development and optimization of a binding assay for the XIAP BIR3 domain using fluorescence polarization. Anal Biochem 2004;332:261–73. [PubMed: 15325294]

24. Peng Y, Sun H, Wang S. Design and synthesis of a 1,5-diazabicyclo[6,3,0] dodecane amino acid derivative as a novel dipeptide reverse-turn mimetic. Tetrahedron Letters 2006;47(27):4769–4770.
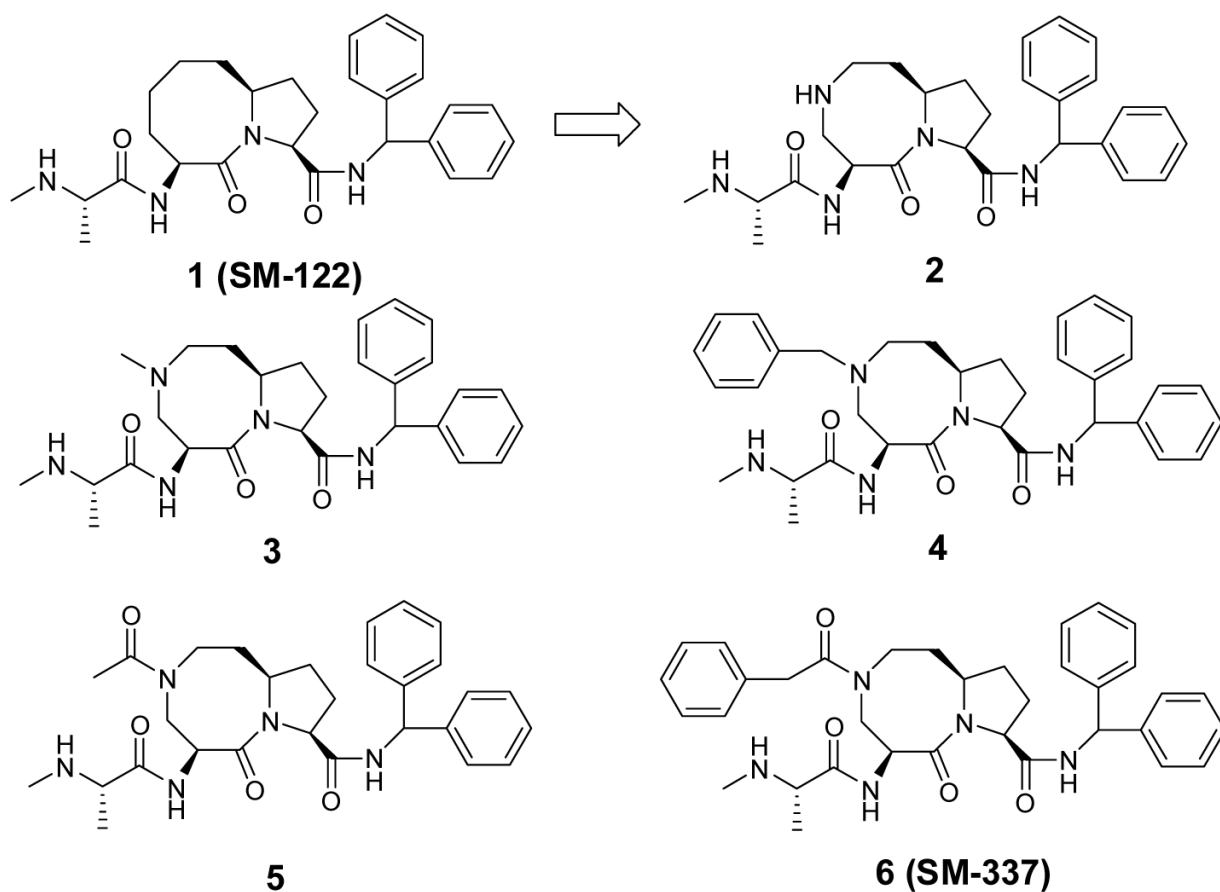
Figure 1.
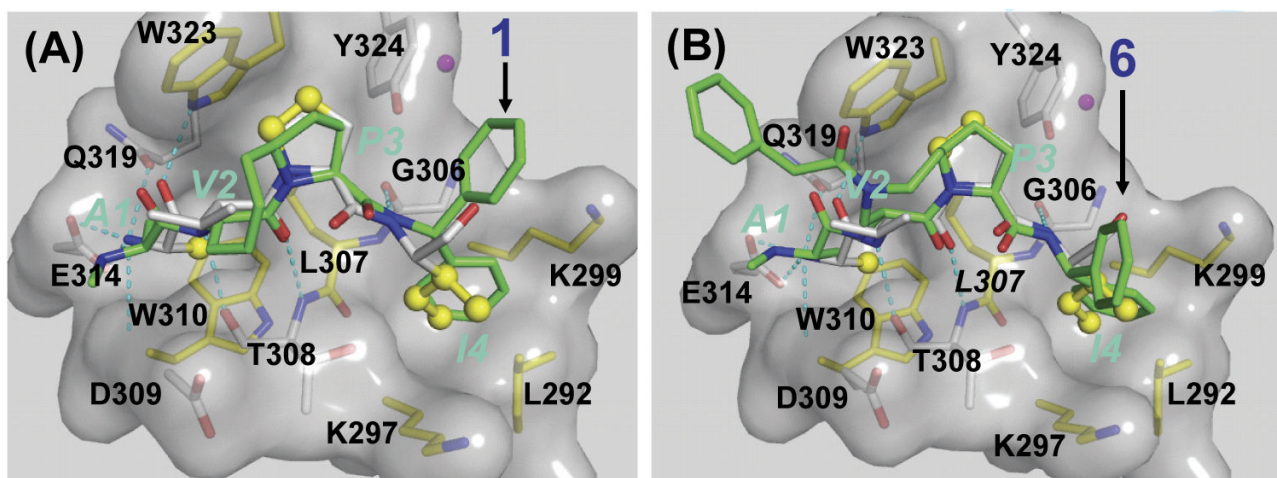Chemical structures of designed Smac mimetics

Figure 2.
Predicted binding models of compounds **1** and **6** to XIAP BIR3 domain, in superposition with Smac AVPI peptide. Compounds **1** and **6** are colored in green and the AVPI peptide in yellow. Binding pockets are shown in transparent surface. Oxygen, nitrogen, sulfur atoms are colored in red, blue, and yellow respectively. Hydrogen bonds are depicted in dash lines.
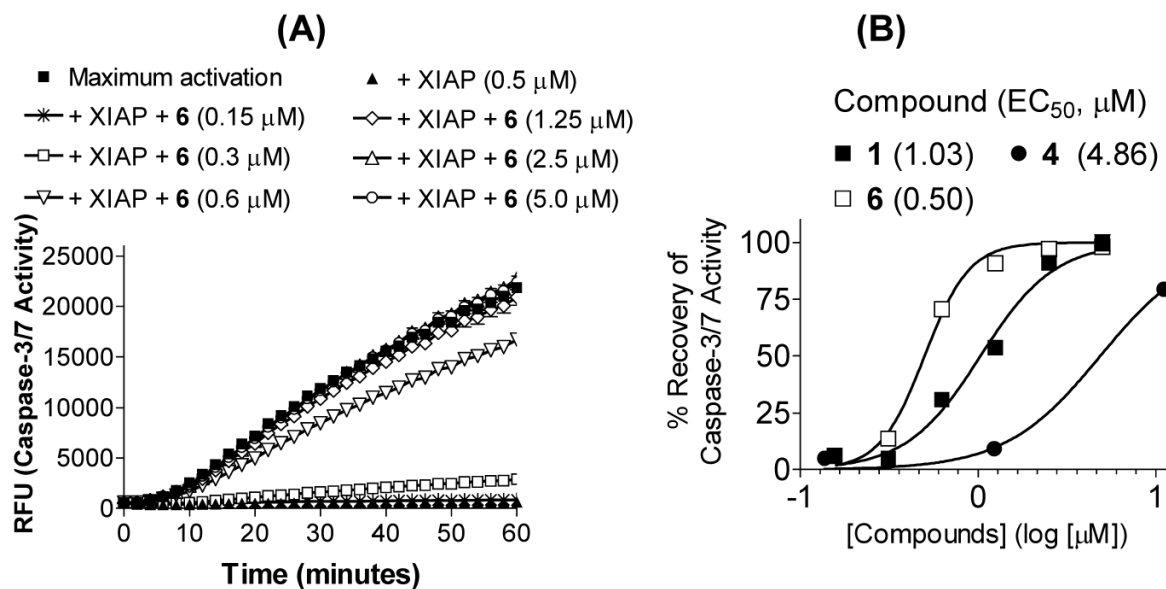
(A)

- ■ Maximum activation
- ──✳── + XIAP + **6** (0.15 μM)
- ──□── + XIAP + **6** (0.3 μM)
- ──▽── + XIAP + **6** (0.6 μM)
- ▲ + XIAP (0.5 μM)
- ──◇── + XIAP + **6** (1.25 μM)
- ──△── + XIAP + **6** (2.5 μM)
- ──○── + XIAP + **6** (5.0 μM)

(B)

Compound (EC$_{50}$, μM)
- ■ **1** (1.03) ● **4** (4.86)
- □ **6** (0.50)

Figure 3.
Inhibition of caspase-3/-7 activity by XIAP and antagonism of Smac mimetics to XIAP to recover the activity of caspase-3/-7 in a cell-free functional assay. (A). Caspase-3/-7 was activated by addition of cytochrome c and dATP into cell lysates and recombinant XIAP BIR3 protein at 0.5 μM completely inhibited caspase activation. Compound **6** dose-dependently recovered the caspase-3/-7 activity. (B). Dose-dependent recovery of caspase-3/-7 activity by **1**, **4** and **6** to the maximum activation. Caspase-3/-7 activity at 30 minute time point was used.
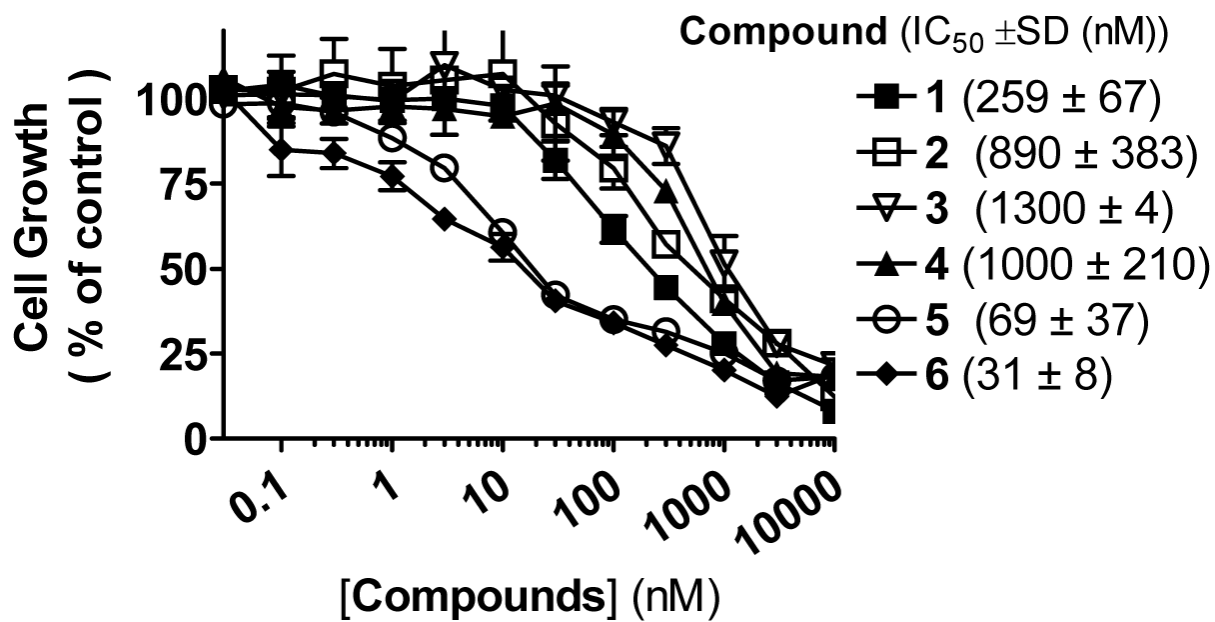
Figure 4.
Inhibition of cell growth by Smac mimetics in the MDA-MB-231 cancer cell line. Cells were treated with Smac mimetics for 4 days and cell growth was determined using a WST-based assay.
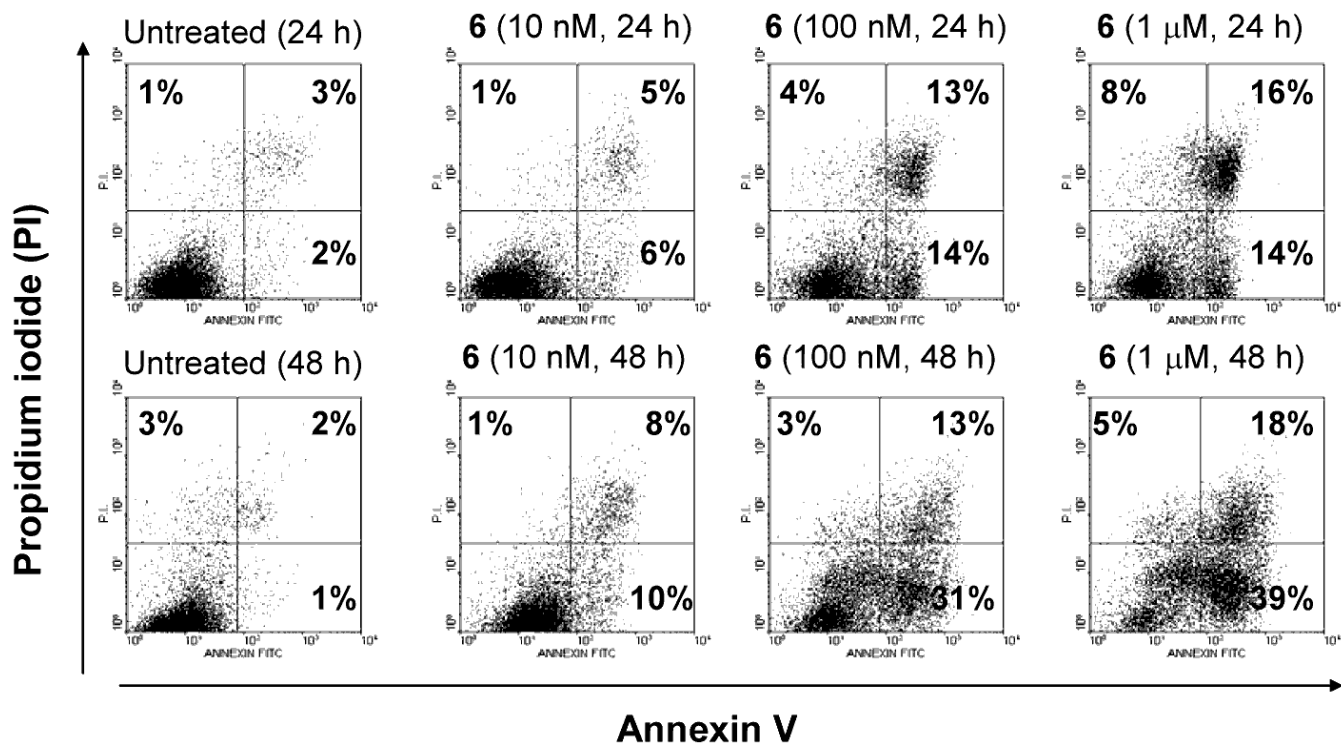
Figure 5.
Induction of apoptisis by compound **6** in the MDA-MB-231 cell line. Cells were treated with different concentrations of **6** for 24 or 48 hours. Apoptosis was analyzed using Annexin V and propidium iodide double staining by flow cytometry. Percentage of early apoptotic (Annexin V+/PI-), late apoptotic (Annexin V+/PI-) and dead (Annexin V+/PI-) cells, are shown, respectively.
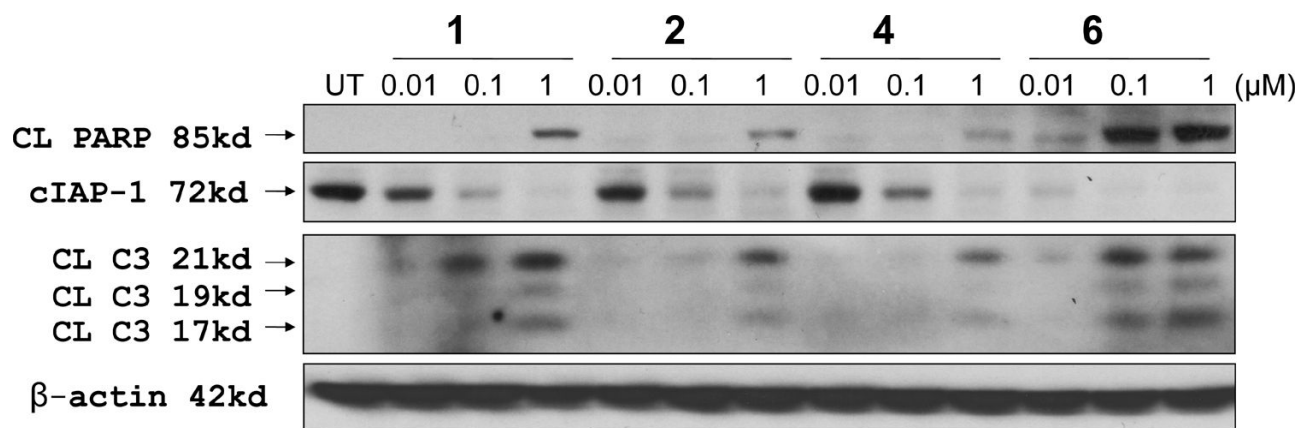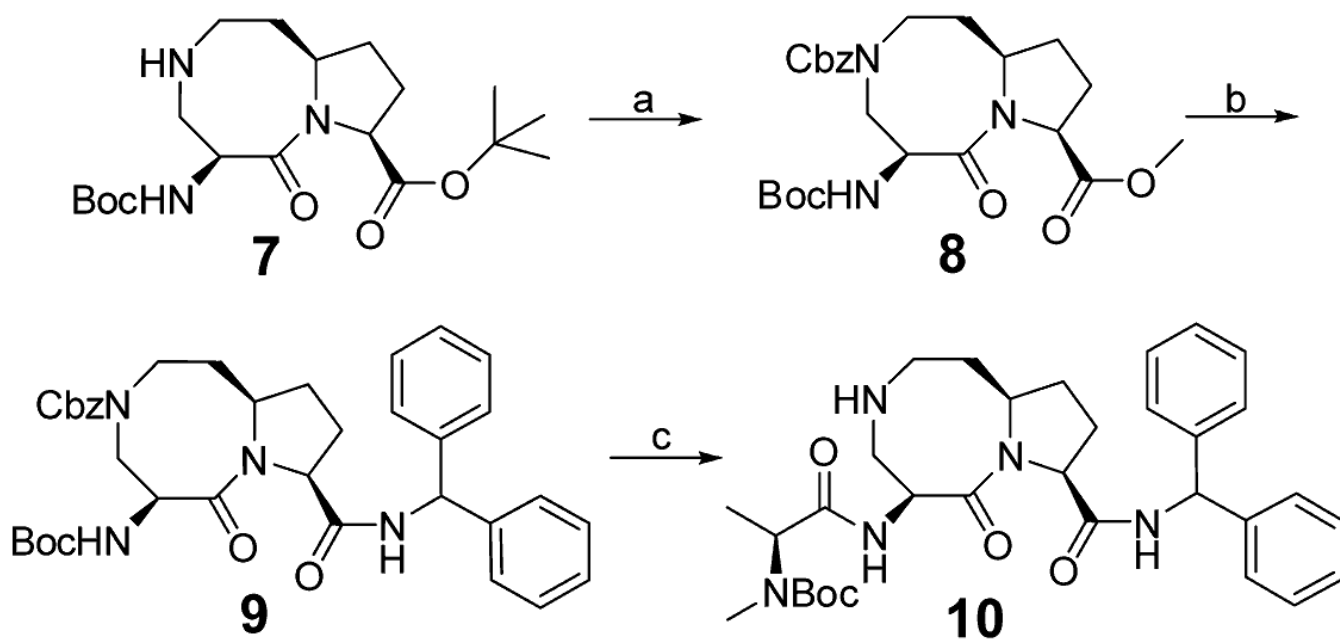
Figure 6.
Induction of cIAP-1 degradation, cleavage of PARP and processing of caspase-3 by compounds **1**, **2**, **4** and **6** in the MDA-MB-231 cell line. Cells were treated with different concentrations of Smac mimetics for 24 hours and levels of cIAP-1, cleaved PAPR (CL PARP), cleaved caspase-3 (CL C3) were probed by Western blot.

Scheme I.
Synthesis of the key intermediate **10**.
Reagents and conditions: (a) i. CbzCl, NaHCO₃, 1,4-dioxane, rt, overnight; ii. SOCl₂, methanol, rt, overnight; iii. (Boc)₂O, NaHCO₃, 1,4-dioxane, rt, overnight, 65% over three steps; (b) i. 2 N LiOH, 1,4-dioxane, 3 hours, then 1 N HCl; ii. aminodiphenylmethane, EDC, HOBt, *N,N*-diisopropylethylamine, rt, overnight, 82% over two steps; (c) i. 4 N HCl in 1,4-dioxane, methanol, rt, overnight; ii. L-*N*-Boc-*N*-methyl-alanine, EDC, HOBt, *N,N*-diisopropylethylamine, rt, overnight; iii. H₂, 10% Pd-C, methanol, overnight, 77% over three steps.

10 $\xrightarrow{a}$ 2   10 $\xrightarrow{b}$ 3

10 $\xrightarrow{c}$ 4   10 $\xrightarrow{d}$ 5, 6
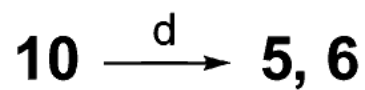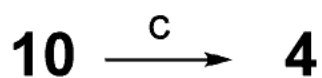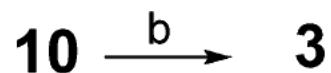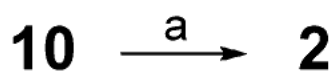
Scheme II.
Synthesis of designed Smac mimetics.
Reagents and conditions: (a) 4 N HCl in 1,4-dioxane, methanol, rt, overnight, 95%; (b) i. formaldehyde (37% in water), NaBH$_3$CN, HOAc, methanol, rt, overnight; ii. 4 N HCl in 1,4-dioxane, methanol, rt, overnight, 71% over two steps; (c) i. BnBr, NaHCO3, 1,4-dioxane, rt, overnight; ii. 4 N HCl in 1,4-dioxane, methanol, rt, overnight, 77% over two steps; (d) i. Ac$_2$O or BnCOCl, *N,N*-diisopropylethylamine, CH$_2$Cl$_2$, rt, overnight; ii. 4 N HCl in 1,4-dioxane, methanol, rt, overnight; 85% for **5** and 87% for **6** over two steps.

Table 1

Binding affinities of Smac mimetics to XIAP, cIAP-1 and cIAP-2, as determined in competitive, fluorescence-polarization based assays (assays details provided in SI). Data were obtained using 3-5 independent experiments.

Cpds	$K_i \pm SD$ (nM)		
	XIAP	**cIAP-1**	**cIAP2**
1	26 ± 4	1.0 ± 0.3	1.8 ± 0.6
2	20.0 ± 14.5	1.2 ± 0.1	4.6 ± 1.5
3	341 ± 65.9	3.3 ± 1.3	17.5 ± 4.3
4	91.8 ± 30.4	3.7 ± 1.4	9.8 ± 4.1
5	5.4 ± 3.0	1.3 ± 0.3	1.9 ± 0.8
6	8.4 ± 1.6	1.5 ± 0.5	4.2 ± 0.6